HIGH POWER LASER
SCIENCE AND ENGINEERING

RESEARCH ARTICLE

A novel cleanliness control method for disk amplifiers

Yangshuai Li[1], Bingyan Wang[1], Panzheng Zhang[1], Yanli Zhang[1], Yanfeng Zhang[1], Shenlei Zhou[1],
Weixin Ma[2], and Jianqiang Zhu[1]

[1] *Key Laboratory on High Power Laser and Physics, Shanghai Institute of Optics and Fine Mechanics, Chinese Academy of Sciences, Shanghai 201800, China*

[2] *Shanghai Institute of Laser Plasma, China Academy of Engineering Physics, Shanghai 201800, China*

Abstract

As the key part for energy amplification of high-power laser systems, disk amplifiers must work in an extremely clean environment. Different from the traditional cleanliness control scheme of active intake and passive exhaust (AIPE), a new method of active exhaust and passive intake (AEPI) is proposed in this paper. Combined with computational fluid dynamics (CFD) technology, through the optimization design of the sizes, shapes, and locations of different outlets and inlets, the turbulence that is unfavorable to cleanliness control is effectively avoided in the disk amplifier cavity during the process of AEPI. Finally, the cleanliness control of the cavity of the disk amplifier can be realized just by once exhaust. Meanwhile, the micro negative pressure environment in the amplifier cavity produced during the exhaust process reduces the requirement for sealing. This method is simple, time saving, gas saving, efficient, and safe. It is also suitable for the cleanliness control of similar amplifiers.

Keywords: active exhaust and passive intake; computational fluid dynamics; cleanliness control; disk amplifier

1. Introduction

As the key part for energy amplification of high-power laser systems, disk amplifiers are responsible for more than 99.9% of energy amplification. Cleanliness is one of the key factors that determine the operation efficiency and life of the amplifiers. Therefore, it is especially important to achieve cleanliness control of the amplifiers[1–3]. The traditional cleanliness control method of the disk amplifiers is 'active intake + passive exhaust' (AIPE)[4–9]. This method uses clean air or nitrogen as a clean purge gas at a certain pressure. Owing to the particularity of the amplifier structure, it is easy to cause turbulence during the process of AIPE. As a result, the contamination floating with the airflow is difficult to exclude from the amplifier cavity. To completely realize cleanliness control, the most common method is to extend the intake and exhaust times. This method is time consuming and gas consuming. In addition, the use of high-pressure gas (one or two standard atmospheric pressures) in this method, generates certain requirements for the sealing of the amplifier

cavity. Later, in order to achieve the cleanliness control of the amplifier, the method of intermittent multiple active intake and passive exhaust (IMAIPE) was developed[10], that is, the pollutant concentration was diluted by multiple and intermittent intake and exhaust. Finally, the amplifier cavity is clean. Similarly, this method of IMAIPE is also time consuming, gas consuming, and also has some problems and risks caused by high gas pressure. In order to realize the cleanliness control of the amplifier cavity at one time, based on the original cleanliness control method of AIPE, through the reasonable design of air inlets and outlets of different amplifiers, Ren *et al.*[11,12] realized cleanliness control with almost no turbulence. His findings also indicate that the amplifier cavity can quickly achieve cleanliness control without turbulence. However, this method also uses high-pressure gas directly in the amplifier cavity, without the secondary partial pressure of the gas chamber. The high pressure brings great danger. This method increases gas consumption and is not operable.

Therefore, how to design the flow field with low pressure and little turbulence is the key to realizing cleanliness control of the amplifier at one time. Based on the above factors, a novel cleanliness control method of active exhaust and

Correspondence to: Jianqiang Zhu, 390 Qinghe Road, Jiading District, Shanghai 201800, China. Email: jqzhu@siom.ac.cn

1

passive intake (AEPI) is proposed in this paper. Combined with computational fluid dynamics (CFD) technology, through the optimization design of inlets and outlets, little turbulence is generated during the process of AEPI. Finally, the cleanliness control of the disk amplifier is realized at one time. At the same time, atmospheric pressure is used for intake and exhaust (tens to hundreds of Pascals below the standard atmospheric pressure), so the maximum pressure drop in the amplifier cavity is only a few thousand Pascals. Thus, the requirements for sealing the amplifier and the risk of damage to the blast shield glass are greatly reduced.

2. Control method and model verification

2.1. Introduction to AEPI and CFD technology

In Figure 1, two different cleanliness control methods are shown: the solid line represents active mode and the dotted line represents passive mode. Different from the traditional cleanliness control method of AIPE (Figure 1(a)), the AEPI is a combination of active exhaust and passive intake (Figure 1(b)). Outlets are usually connected to a negative pressure device (such as a high-power exhaust fan) and inlets are connected to atmospheric gas (such as clean nitrogen or clean air). Combined with the optimization design of inlets and outlets, the negative pressure pumping (exhaust) actively guides the direction of gas flow through the amplifier cavity. This greatly reduces the probability of turbulence generation and improves the clean purge efficiency. In addition, owing to the active exhaust (pumping), the pressure in the amplifier cavity is slightly lower than normal pressure. Compared with the traditional active intake of high pressure and passive exhaust, the requirement for sealing of the amplifier cavity in the AEPI method is lower. With the presence of negative pressure, the amplifier is better sealed (self-pressing principle).

CFD[13,14] is widely used in the numerical simulation of gas flow. First, it discretizes the hydrodynamic equations followed by the air flow in the calculation domain, transforms the strongly nonlinear partial differential equations into algebraic equations, and then uses certain numerical calculation technology to solve them, so as to obtain detailed
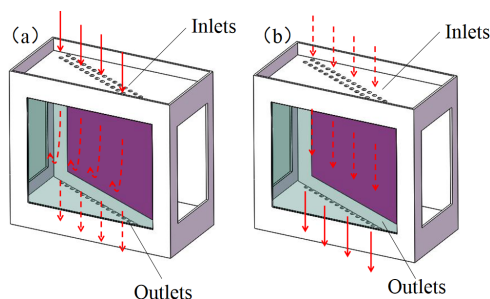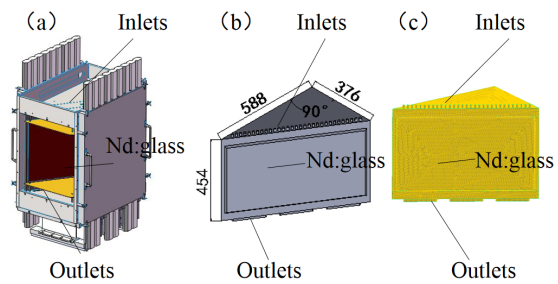

**Figure 2.** (a) The configuration of SSA; (b) the calculation model; (c) the mesh generation.

information of the flow field distribution in the whole calculation region. Finally, the results can be visualized by computer graphics technology. Generally speaking, CFD usually includes the following steps: establishing mathematical and physical model (pre-processing), numerical algorithm solving, and result visualization (post-processing).

2.2. Numerical calculation model and governing equations

Taking one type of single-aperture slab amplifier (SSA) in the National Laboratory of High Power Laser and Physics (NLHPLP) as an example, half of the amplifier cavity was chosen as the model for checking numerical calculations (Figure 2), because the structures on both sides of neodymium glass (Nd:glass) are the same. The model mainly includes inlets, outlets, and Nd:glass. The air inlets are composed of a row of small holes with a diameter of 10 mm, and the air outlets at the opposite position of the inlets are composed of three elongated holes with a width of 10 mm. The method of combining Tet/Hybrid element with TGrid is used for mesh generation. To obtain suitable mesh generation, three kinds of mesh numbers are divided according to the size of the grid. The mesh densities of inlets and outlets are optimized locally. The simulation results show that the internal pressure and flow state of the amplifier are basically the same under the three grid sizes, so to save calculation time, the final mesh number of 1,357,773 was chosen.

Similarly, to simplify the calculation model, we assumed that: (1) the thermal characteristics of the fluid are stable; (2) the flow state of the fluid is determined by the Reynolds number at the suction port speed; (3) the aerosol particles in the amplifier cavity are small enough and light enough to flow with clean gas. Therefore, the flow field can represent the distribution of aerosol particles.

The basic equations of fluid analysis and turbulent flow were used as the control equations[14]. These basic equations include the equations for the conservation of mass, momentum, and energy. The turbulent flow model is the RNG k-ε model. The default values of the software were used for the relevant parameters.

**Figure 1.** Cleanliness control methods: (a) AIPE; (b) AEPI.
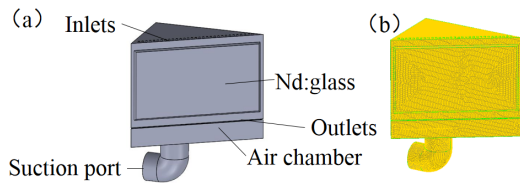
Figure 3. (a) The modified model; (b) the mesh generation of the modified model.

As it is difficult to guarantee the same speed of the air outlets during the experimental verification process, we separately added the air chamber under and connecting with outlets on the basis of the original model to strictly approximate and facilitate real experimental verification. The newly improved experimental model is shown in Figure 3. The related parameter settings and process are similar to the previous model.

2.3. Numerical model verification

To verify the correctness of the numerical calculation model, the modified SSA cavity structure shown in Figure 4 is adopted. It is strictly the same as the modified theoretical model in Figure 3, including inlets, outlets, and neodymium glass cavity. To allow the flow field in the cavity to be seen, PVC was used instead of neodymium glass. The inner wall of the cavity is covered with black paper. The experiment was carried out in a dark room.

The suction port is connected to a high-power fan[15] (model MF-150P), which can realize a pumping speed of 360–530 m^3/h. The suction port is connected to the air chamber, which in turn is connected with outlets. When the exhaust fan starts to work, an active air extraction speed of 20–30 m/s at the outlets can be realized (20 m/s was selected in this experiment). The air inlets connected to the external atmosphere consist of a series of 10 mm diameter holes evenly distributed along the edge. A pressure gauge is placed in the modified SSA cavity to measure the internal pressure. Three smoke cakes[16] were placed near air inlets, and the smoke they produced accompanied the air into the amplifier cavity. By monitoring the fluid state of smoke in the amplifier
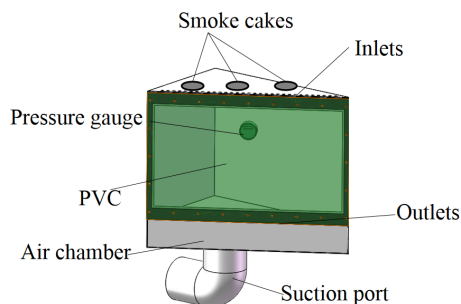
Figure 4. The modified SSA cavity.

cavity, the flow field in the amplifier is characterized, and then the pollutant removal efficiency is reflected[12]. The steady-state flow field in the amplifier cavity was recorded. The correctness of the theoretical simulation is verified by comparing the experiment with the theory.

3. Results and discussion

### 3.1. Theoretical simulation and experimental results

Using the AEPI method, the intake air speed is 20 m/s. The theoretical and experimental results obtained are shown in Figures 5 and 6. The pressures in the figures are relative to standard atmospheric pressure. It can be seen from Figures 5(a) and 5(b) that under the experimental parameter conditions, the pressure within the entire modified SSA cavity is between –2000 and 2000 Pa (relative to standard atmospheric pressure). In Figure 5(c), the experimental results are 0 Pa in the position of the bottom surface of the cavity and –113 Pa in the position of outlets, which are relatively consistent with the theoretical results.

Therefore, based on the above experimental and theoretical results, we believe that the CFD model is correct and the internal pressure of the amplifier cavity obtained by AEPI method is very small. To minimize turbulence, it is necessary to further optimize the SSA cavity structure and air exhaust velocity.

3.2. Design optimization

For the SSA amplifier, to achieve the goal minimal turbulence, some optimization designs of the inlets, outlets, and speeds of air exhaust have been made. We set up a series of circular inlets and rectangular outlets along the other two sides of the triangle, with different air exhaust speeds (20, 40, and 80 m/s). The final results are shown in Figure 7. When the speed is 20 or 40 m/s, two huge eddies are generated along the two acute angles of the triangle, so it is hard to remove pollutants. When the speed reaches 80 m/s, there is only a small vortex, and then the SSA cavity can be quickly cleaned. The pressure in the cavity is very low. Therefore, using the amplifier cavity structure shown in Figure 2 and an exhaust speed of 80 m/s, the cleanliness of the SSA cavity can be controlled effectively.

In addition to SSAs, the method of AEPI is also applicable to multi-segment disk amplifiers (MSAs). Taking one type of MSA as an example, its structure is shown in Figure 8. Similarly, we choose the 1/4 structure. The simplified figure is shown in Figure 8(b). A series of circular inlets and outlets are provided along the three sides of the triangle. The exhaust speeds used are 10, 20, 40, and 80 m/s. The final results are shown in Figures 9 and 10. The results show that under the condition of exhaust speeds of 10 or 20 m/s,
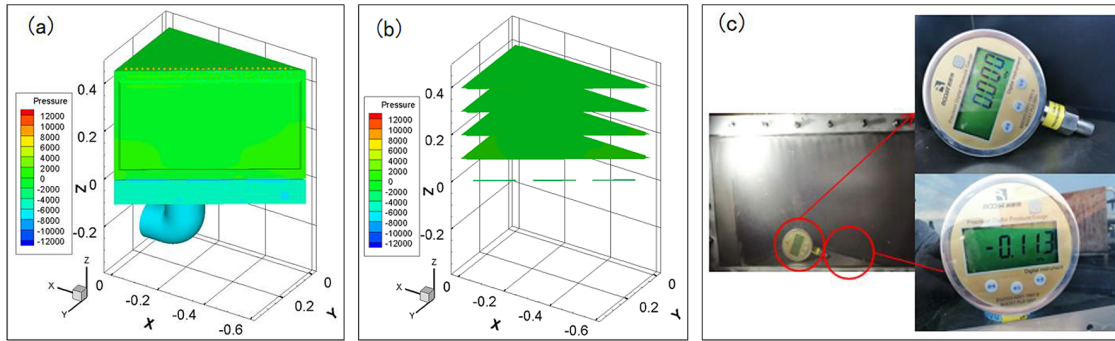
Figure 5. Pressure in the modified SSA cavity: (a) pressure of the whole cavity; (b) pressures in the positions of $Z = 0, 0.1, 0.2, 0.3$ and 0.4 m; (c) experimental result.
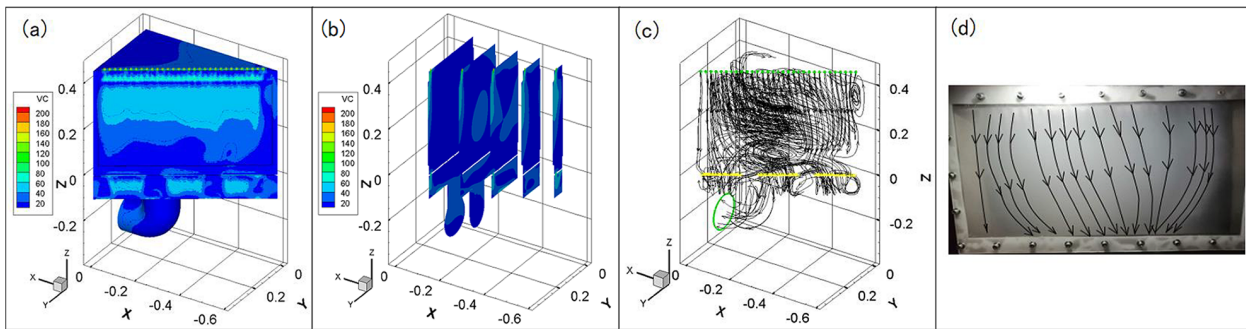
Figure 6. The flow field in the modified SSA cavity in steady state: (a) contour of velocity; (b) slices of velocities in different positions; (c) vector of velocity; (d) experimental result.
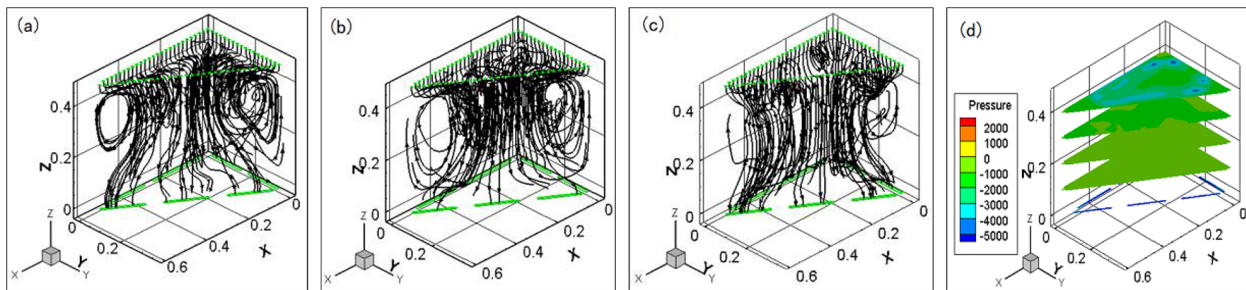

Figure 7. Vectors of different pump speeds and pressures: (a) 20 m/s; (b) 40 m/s; (c) 80 m/s; (d) 80 m/s.

two larger vortexes are generated in the direction of the two acute angles close to the triangle. As the exhaust speed increases (40 and 80 m/s), the vortex gradually decreases and disappears. Although Figure 9(d) produces a vortex in the direction close to the air inlet, the vortex is small, and the vortex will instead bring out the pollutants in the sharp corners, so cleanliness control can also be well achieved. In addition, at exhaust speeds of 40 and 80 m/s, the pressures in the amplifier cavity are also small. Therefore, MSA can achieve cleanliness control by adopting the AEPI method and reasonable structure design.

4. Conclusion

Regarding the amplifier, a new cleanliness control method of AEPI has been proposed. Taking one type of disk amplifier
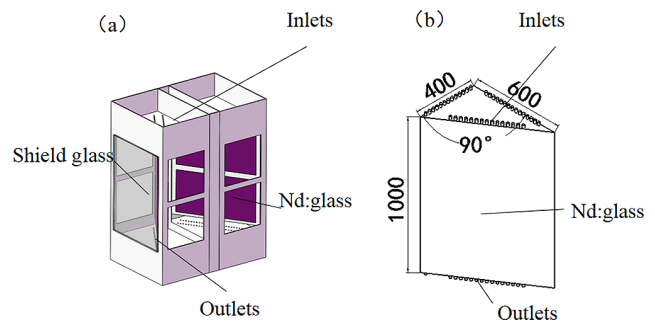
Figure 8. (a) The configuration of MSA; (b) the calculation model.

as the research object, a cleanliness control model based on CFD technology has been established and verified. Based on this new cleanliness control method, optimization designs for cleanliness control in SSAs and MSAs were conducted.
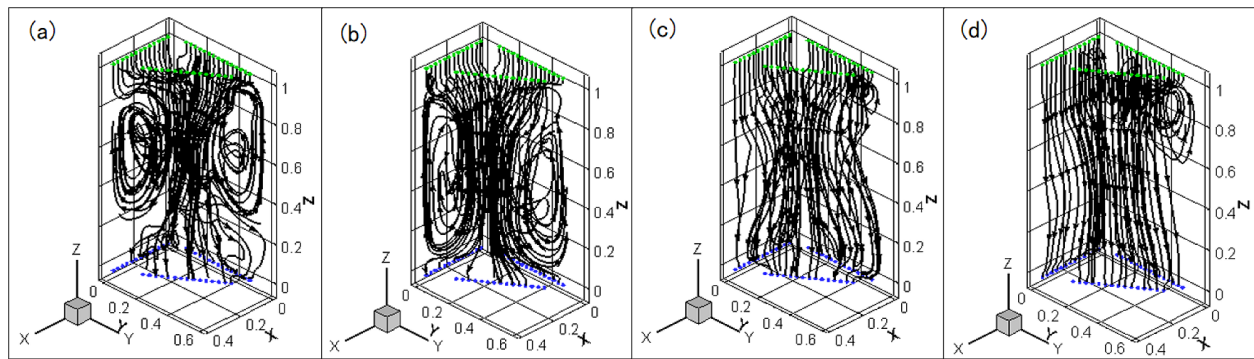
Figure 9. Vectors at different air speeds in the outlets: (a) 10 m/s; (b) 20 m/s; (c) 40 m/s; (d) 80 m/s.
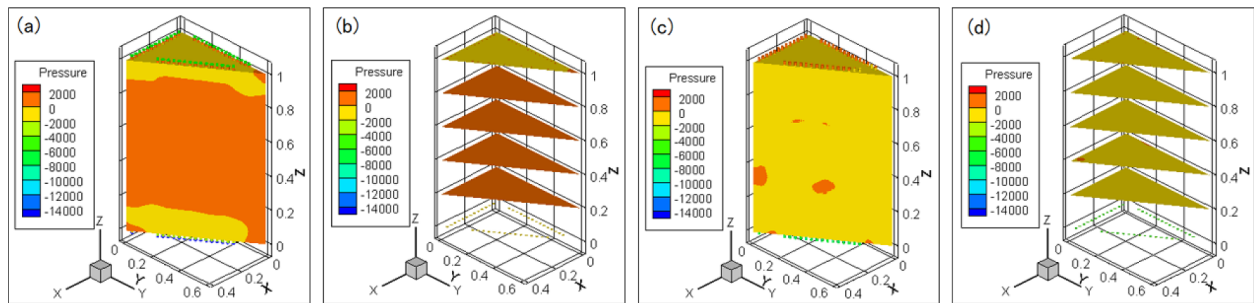

Figure 10. Pressures at different air speeds in the outlets: (a) 40 m/s; (b) 40 m/s; (c) 80 m/s; (d) 80 m/s.

The research results show that it is feasible and effective to use the AEPI to achieve cleanliness control of the amplifier. The method can realize the cleanliness control of the disk amplifier by exhausting gas at one time, and also reduces the requirement of sealing the amplifier cavity. It has the advantage of time saving, gas saving, and safety and is suitable for cleanliness control of the same type of disk amplifier. It is also expected that this method could be used to realize the windowless design of the main amplification system. Of course, the flow field also involves the cooling of neodymium glass, and we will carry out this work in the next step. We also believe that there will be more efficient methods or structures for clean control of amplifiers in the future.

Acknowledgment

References

1. Y. Li, "Cleanliness control technology of high power laser systems", PhD Thesis (University of Chinese Academy of Sciences, 2015).
2. M.-C. Jiang, J.-Q. Zhu, Z.-G. Liu, and L. Wang, Acta Photon. Sin. **45**, 1114001 (2016).
3. Y.-S. Li, B.-Y. Wang, P.-Z. Zhang, Z.-Y. Ren, Z.-G. Liu, S.-L. Zhou, W.-X. Ma, J. Zhu, and J.-Q. Zhu, Proc. SPIE **10748**, 107480Y (2018).
4. I. F. Stowers, J. A. Horvath, J. A. Menapace, A. K. Burnham, and S. A. Letts, Proc. SPIE **3492**, 609 (1998).
5. H.-W. Yu, W.-G. Zheng, J. Tang, C.-C. Wang, Y. Liu, S.-B. He, X.-F. Wei, and X.-M. Zhang, High Power Laser Part. Beams **13**, 272 (2001).
6. M. L. Spaeth, K. R. Manes, and J. Honig, Fusion Sci. Technol. **69**, 250 (2016).
7. J. A. Paisner, W. H. Lowdermilk, J. D. Boyes, M. S. Sorem, and J. M. Soures, Fusion Eng. Des. **44**, 23 (1999).
8. J. Honig, Opt. Eng. **43**, 2904 (2004).
9. X.-F. Cheng, X.-X. Miao, Y.-B. Chen, H.-B. Wang, L. Qin, H.-B. Lu, Q. Xiong, Q. He, Z.-Q. Ma, Y.-Y. Ye, L.-B. Zhao, Y. Liu, S.-B. He, X.-D. Yuan, Q.-H. Zhu, F. Jing, and W.-G. Zheng, High Power Laser Part. Beams **24**, 1 (2012).
10. P.-Z. Zhang, T. Feng, J. Xie, Z.-Y. Ren, X.-W. Yang, L. Wang, J.-H. Li, Z.-X. Zhang, Z.-D. Cao, Z.-Q. Xia, J.-F. Hu, Z.-H. Chai, Z.-G. Liu, S.-L. Zhou, W.-X. Ma, and J. Zhu, Chin. J. Lasers **45**, 0401014 (2018).
11. X.-W. Yang, Z.-G. Liu, Z.-Y. Ren, H.-Q. Zhang, and J.-Q. Zhu, Chin. J. Lasers **43**, 0901002 (2016).
12. Z.-Y. Ren, J.-Q. Zhu, Z.-G. Liu, and X.-W. Yang, High Power Laser Sci. Eng. **6**, e1 (2018).
13. Y.-S. Li, J.-Q. Zhu, X.-Y. Pang, H. Tao, X. Jiao, and Y.-Z. Wu, High Power Laser Sci. Eng. **3**, e5 (2015).
14. F.-J. Wang, *Computational Fluid Dynamics Analysis—CFD Software Principles and Application* (Tsinghua University Press, Beijing, 2004).
15. https://detail.tmall.com/item.htm?id=575437747923&spm=a1z09.2.0.0.46a62e8dOdsKMh&_u=6e56n20032d
16. https://detail.tmall.com/item.htm?id=596215712252&spm=a1z09.2.0.0.67002e8dVQwyWQ&_u=de56n2073e2